18th Australasian Fluid Mechanics Conference

Launceston, Australia

3-7 December 2012

Numerical analysis of peristaltic pump in a curved microchannel considering non-Newtonian flow and magnetic field

A. Kalantari[1], S. Toosi[1], A. Riasi[1] and K. Sadeghy[1]

[1]School of Mechanical Engineering, College of Engineering, University of Tehran

P.O.Box: 11155-4563, Tehran, Iran

Abstract

The peristaltic flow of non-Newtonian fluid in a curved micro-channel is investigated in this paper. The channel is assumed to have a radial magnetic field and second order velocity slip on walls. Non-Newtonian behaviour is described using both third-order and Giesekus models. Assuming long wavelength for walls' motion, governing equations can be reduced to a nonlinear system of ODEs in low Reynolds number regime. Both spectral-Galerkin and finite difference methods are implemented to solve the governing equations, with results showing to have good agreement together. For a constant flow rate, shear thinning (thickening) behaviour of fluid causes a lower (greater) pressure rise in the stream wise direction. In pumping region, curvature increases the stream wise pressure difference for low flow rates; while it has a reverse effect in co-pumping region. The maximum of the velocity profile moves towards the inner wall with increase in curvature or Knudson number. However, the effect of magnetic field is to flatten the velocity profile, and hence to enhance the peristalsis pumping rate.

Introduction

The peristaltic flow of Newtonian and non-Newtonain fluid have been studied by many researchers because of its application in physiology and industry. However, only few papers have been devoted to the peristaltic flow in a curved channel. Sato et al [1] have discussed the peristaltic flow of Newtonian flow in a curved channel. Ali et al [2] have examined the peristaltic flow of third order fluid in a curved channel. The aim of this paper is to study the behavior of third grade and Giesekus fluid considering the effect of magnetic field and slip condition.

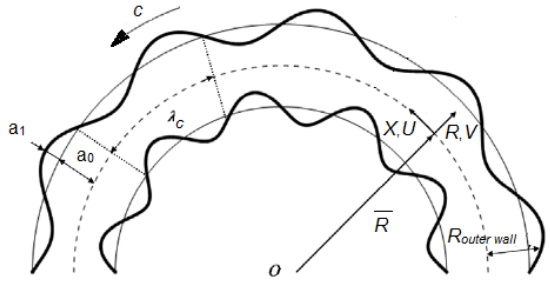

Figure 1. Schematic showing the flow geometry

Mathematical Formulation

Consider a deformable curved channel with radius of $\bar{R}$ and width of $2a_0$ in which a wave propagates along the walls at constant speed of c(see figure 1). The flow field is subjected to a magnetic field varying in radial direction. The vertical displacements of the walls are as follows:

$$R(X,t)_{Outer\ wall} = a_0 + a_1 sin\left(\frac{2\pi}{\lambda_c}(X - ct)\right) \quad (1)$$

$$R(X,t)_{Inner\ wall} = -a_0 - a_1 sin\left(\frac{2\pi}{\lambda_c}(X - ct)\right) \quad (2)$$

Where a_1 is the amplitude of the peristaltic wave, λ_c is the peristaltic wavelength, and t and X are time and tangential coordinate respectively. The flow is assumed to be incompressible and laminar, with no component in the z-direction. Representing the components of velocity vector $\vec{\boldsymbol{V}}$ by $V(R,X,t)$ and $U(R,X,t)$ in the radial and tangential directions respectively, the Cauchy equation of motion together with the continuity equation for a MHD fluid reads [3]:

$$div(\boldsymbol{V}) = 0 \quad (3)$$

$$\rho\left(\frac{D\boldsymbol{V}}{Dt}\right) = -\nabla p + div(\tau) + J \times B_R, J = \sigma_e(E + \boldsymbol{V} \times B_R) \quad (4)$$

Where p is the fluid pressure, τ is stress tensor, ρ is the density, J is the current density, σ_e is electrical conductivity, E is electric field and B_R is radial magnetic field varying proportional to $1/R$. Assuming that the magnetic Reynolds number is sufficiently small, the motion induced magnetic and electric fields can safely be neglected. This assumption is employed in the following.

The stress tensor is related to the velocity field using constitutive equations, defined by non-Newtonian model implemented. In this paper non-Newtonian behavior is described using both third order and Giesekus models. For the third order flow the constitutive equation is represented as:

$$\tau = \eta A_1 + \alpha_1 A_2 + \alpha_2 A_1^2 + \beta_1 (tr A_1^2) A_1 \quad (5)$$

Where η is the fluid viscosity. α_1, α_2 and β_1 are material parameters, named retarded-motion constants. A_1 and A_2 are Rivlin-Ericson tensors defined as:

$$A_1 = 2D = \nabla V + (\nabla V)^T \quad (6)$$

$$A_n = \frac{DA_{n-1}}{Dt} + A_{n-1}.(\nabla V) + (\nabla V)^T.A_{n-1} \quad (7)$$

In above equation D/Dt is material derivative and D is the rate of deformation tensor. The third order model is reliable only under assumptions of small velocity gradient and slow flow, which are necessity of retarded motion expansion. To eliminate these restrictions, the Giesekus model is implemented in this paper [4]:

$$\tau + \frac{\alpha\lambda}{\eta}(\tau.\tau) + \lambda\left(\frac{D\tau}{Dt} - (\tau.(\nabla V) + (\nabla V)^T.\tau)\right) = 2\eta D \quad (8)$$

Here α and λ are the mobility factor and relaxation time, respectively. The Giesekus model is regarded as one of the best rheological models to represent polymer liquids. This is because it correctly predicts shear thinning, non-vanishing first and second normal stress differences, finite extensional viscosity and non-exponential stress relaxation or stress growth curve for polymer liquids. It is imperative to say that the mobility factor should be selected in the range of $0 \leq \alpha \leq 0.5$ in spite of the fact that it can be increased to one from theoretical point of view. In the current coordinate the flow is unsteady. However, using a transformation it can be considered as steady in a wave frame coordinate. Transformation equations are:

$$(x = X - ct, r = R), \qquad (u = U - c, v = V) \tag{9}$$

Introducing following dimensionless parameters:

$$v^* = \frac{v}{c\delta}, u^* = \frac{u}{c}, x^* = \frac{2\pi x}{\lambda}, r^* = \frac{r}{a_0}, \tau^* = \frac{a_0}{c\eta}\tau, p^* = \frac{a_0\delta}{c\eta}p,$$
$$k = \frac{\bar{R}}{a_0}, Re = \frac{\rho c a_0}{r}, \frac{B_r}{B_0} = \frac{1}{r+k}, M = \sqrt{\frac{\sigma_e}{\eta}}B_0 a_0, \delta = \frac{2\pi a_0}{\lambda} \tag{10}$$

Where, k is curvature parameter, Re is Reynolds number, M is Hartman number and δ is wavelength ratio, and having dropped "*" the dimensionless form of continuity and Cauchy equations are transfigured to:

$$Re.\delta\left(-\delta^2\frac{\partial v}{\partial x} + \delta^2 v\frac{\partial v}{\partial r} + \delta^2\frac{k(u+1)}{r+k}\frac{\partial v}{\partial x} - \frac{(u+1)^2}{r+k}\right) = -\frac{\partial p}{\partial r} + \left(\frac{\delta}{r+k}\right)\frac{\partial}{\partial r}\{(k+r)\tau_{rr}\} + \delta^2\frac{k}{r+k}\frac{\partial \tau_{rx}}{\partial x} - \left(\frac{\delta}{r+k}\right)\tau_{xx} \tag{11}$$

$$Re.\delta\left(-\frac{\partial u}{\partial x} + v\frac{\partial u}{\partial r} + \frac{k(u+1)}{r+k}\frac{\partial u}{\partial x} + \frac{(u+1)v}{r+k}\right) = -\left(\frac{k}{r+k}\right)\frac{\partial p}{\partial x} + \frac{1}{(r+k)^2}\frac{\partial}{\partial r}\{(r+k)^2\tau_{rx}\} + \delta\left(\frac{k}{r+k}\right)\frac{\partial \tau_{xx}}{\partial x} - M^2\frac{(u+1)}{(r+k)^2} \tag{12}$$

$$\frac{\partial}{\partial r}\{(r+k)v\} + k\frac{\partial u}{\partial x} = 0 \tag{13}$$

Defining stream function as:

$$u = -\frac{\partial \psi}{\partial r}, \qquad v = \frac{k}{r+k}\frac{\partial \psi}{\partial x} \tag{14}$$

And assuming long wavelength for walls' motion ($\delta \to 0$), the equations of motion are reduced to:

$$\frac{\partial p}{\partial r} = 0 \tag{15}$$

$$-\frac{\partial p}{\partial x} + \frac{1}{k(r+k)}\frac{\partial}{\partial r}\{(r+k)^2\tau_{rx}\} - M^2\frac{1-\frac{\partial \psi}{\partial r}}{k(r+k)} = 0 \tag{16}$$

Applying the assumption of long wavelength ratio the constitutive equation of third order model reads:

$$\tau_{rx} = -\frac{\partial^2\psi}{\partial r^2} - \frac{1}{r+k}\left(1 - \frac{\partial \psi}{\partial r}\right) - 2\beta\left(\frac{\partial^2\psi}{\partial r^2} + \frac{1}{r+k}\left(1 - \frac{\partial \psi}{\partial r}\right)\right)^3 \tag{17}$$

Likewise, the constitutive equations of Giesekus model are reduced to:

$$\tau_{rr} + \alpha\, We\, (\tau_{rr}^2 + \tau_{rx}^2) = 0 \tag{18}$$

$$\tau_{rx} - We\,\dot{\gamma}\tau_{xx} + \alpha\, We\,\tau_{rx}(\tau_{rr} + \tau_{xx}) = \dot{\gamma} \tag{19}$$

$$\tau_{xx} - 2\, We\,\dot{\gamma}\tau_{rx} + \alpha\, We\,(\tau_{rx}^2 + \tau_{xx}^2) = 0 \tag{20}$$

Where in the above equations, following dimensionless variables are used:

$$\beta = \frac{\beta_1 C^2}{\eta a_0^2}, \;\; We = \frac{\lambda c}{a_0}, \;\; \dot{\gamma} = (r+k)\frac{\partial}{\partial r}\left(1 - \frac{\partial \psi}{\partial r}\right) \tag{21}$$

To define boundary conditions, the flow rate is represented in wave frame coordinate.

$$\Theta = \int_{R(X,t)_{Inner\,wall}}^{R(X,t)_{Outer\,wall}} U\, dR = \Lambda + 2cR(x,t)_{Outer\,wall} \tag{22}$$

Defining the average flux $\bar{\theta}$ over one period $T = \frac{\lambda}{c}$ of the peristaltic wave and introducing the dimensionless parameters, the final equation is written as:

$$Q = \frac{\bar{\theta}}{a_0 c}, \qquad q = \frac{\Lambda}{a_0 c}, \qquad Q = q + 2 \tag{23}$$

For an isothermal flow the general second-order slip condition has the non-dimensional form [5]:

$$u_s = \frac{2}{2-\sigma_v}\left(C_1 Kn\left(\frac{\partial u}{\partial n}\right) - C_2 Kn^2\frac{\partial^2 u}{\partial n^2}\right) \tag{24}$$

Where $\partial/\partial n$ denotes gradients normal to the wall surface, Kn is Knudson number and σ_v is tangential momentum accommodation coefficient. C_1 and C_2 are slip coefficients. An accurate model can be obtained using $C_1 = 1$ and $C_2 = -0.5$. Hence, the final form of boundary conditions in wave frame, assuming $\sigma_v = 1$, reads:

For $r(x)_{Outer\,wall} = 1 + \phi sin(x)$:

$$\frac{\partial \psi}{\partial r} - Kn\frac{\partial^2\psi}{\partial r^2} - \frac{Kn^2}{2}\frac{\partial^3\psi}{\partial r^3} = 1, \qquad \psi = -\frac{q}{2}, \tag{24}$$

For $r(x)_{Inner\,wall} = -1 - \phi sin(x)$:

$$\frac{\partial \psi}{\partial r} + Kn\frac{\partial^2\psi}{\partial r^2} - \frac{Kn^2}{2}\frac{\partial^3\psi}{\partial r^3} = 1, \qquad \psi = \frac{q}{2} \tag{25}$$

In which $\phi = a_1/a_0$ is called the amplitude ratio.

Method of Solution

Third-Order Model

Combining equation (15) with equation (16) gives:

$$\frac{\partial}{\partial r}\left\{\frac{1}{(r+k)}\frac{\partial}{\partial r}((r+k)^2\tau_{rx})\right\} - M^2\frac{\partial}{\partial r}\left(\frac{1-\frac{\partial \psi}{\partial r}}{r+k}\right) = 0 \tag{26}$$

This ODE looks too formidable to render itself an analytical solution, and hence we look for a numerical procedure to solve this equation. It is necessary to linearize it first before relying on a suitable iterative method for numerical solution. The familiar Newton-Kantorovich method is implemented in order to linearize equation (26) after inserting the equation (17).

The equations (17), (26) along with boundary conditions can be solved numerically using both spectral-Galerkin and finite difference methods. We have tried both methods and found consistent results for each set of independent variables, showing accuracy of numerical procedures. In FDM formulation all derivatives are calculated using second order central difference scheme. The procedure is both familiar and straightforward and then is not repeated here in details. However, the pseudospectral method is

somehow tricky. As the equation is highly nonlinear, the simple use of vanishing residuals on grid points fails to give acceptable results, especially for higher values of β. An alternative way is the use of Galerkin method [6]. In order to use this method we have to first introduce a variable to homogenize the boundary conditions:

$$\Psi(r,x) = \psi(r,x) - ar^3 - cr \tag{27}$$

Where

$$a = \frac{1 - q/(2R)}{4R^2 - 6RKn - 3Kn^2};\ c = aR^2 + \frac{q}{2R};\ R = 1 + \phi\sin(x) \tag{28}$$

Introducing above variable into equation (26), some additional terms are inserted to the right hand side of this equation. Details are eliminated to retain brevity. This new variable Ψ should satisfy homogeneous boundary conditions below:

$$\Psi(\pm R) = 0\,;\quad \frac{\partial\Psi(\pm R)}{\partial r} \mp Kn\frac{\partial^2\Psi(\pm R)}{\partial r^2} - \frac{Kn^2}{2}\frac{\partial^3\Psi(\pm R)}{\partial r^3} = 0 \tag{29}$$

If we expand Ψ using expansion functions each identically satisfying boundary conditions, we can be assure that Ψ satisfies desired boundary conditions:

$$\Psi(r,x) = \sum_{n=1}^{N} a_n(x) f_n(r) \tag{30}$$

Where f_ns are combinations of Chebyshev polynomials, each satisfying boundary conditions:

$$f_n(\eta) = T_n(\eta) + c_1 T_{n+2}(\eta) + c_2 T_{n+4}(\eta) \tag{31}$$

In which:

$$c_1 = -\frac{d_{n+4} - d_n}{d_{n+4} - d_{n+2}}\ ;\quad c_2 = -\frac{d_{n+2} - d_n}{d_{n+2} - d_{n+4}} \tag{32}$$

Where:

$$d_m = m^2 - Kn\frac{m^2(m^2-1)}{3} - \frac{Kn^2}{2}\frac{m^2(m^2-1)(m^2-4)}{15} \tag{33}$$

The first five modes of this function are shown in figure 2.

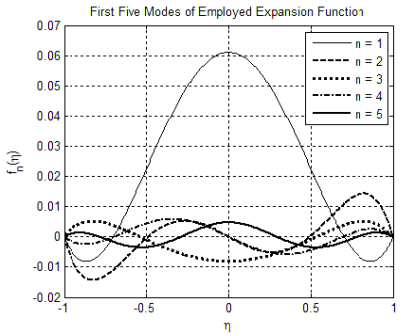

Figure 2. First five modes of the expansion function implemented.

In the Galerkin method we minimize the residuals by forcing it to be orthogonal to base functions in the specified interval. In order to do so, both sides of equation (26) are multiplied by f_m and integrated over the normalized interval of $[-1,1]$ using the appropriate weight function of $1/\sqrt{1-\eta^2}$ (inner product). The resulting matrix equation gives coefficients of expansion functions at each given x.

Giesekus Model

The equations (26) and (18, 19, 20), governing the motion of a Giesekus fluid, cannot be reduced into a single ODE inasmuch as its constitutive equations are implicitly related to the velocity field, rather than explicitly. Indeed, these two equations form a nonlinear system of ODEs that should be solved simultaneously. It should be noted that there is no explicit boundary condition on τ_{rx}, while there are four on the stream function. However, satisfaction of shear stress boundary conditions could be determined by extra boundary conditions on the stream-function. In order to solve this system of equations an iterative method is implemented. The procedure is as follows: The normal stress τ_{rr} is calculated and replaced into these equations using equation (18), as a function of shear stress τ_{rx}. The shear stress, which causes the nonlinearity of the equations, is separated into the two parts ($\tau_{rx} = \tau_{rx}^0 + \tau_{rx}'$). System of equations is discretized using finite difference scheme. An initial guess is made for shear stress field (τ_{rx}^0). Having introduced this stress field into the right hand side of equations (34) and (35), stream-function and shear stress correction are obtained. This procedure is repeated until convergence.

$$(r+k)\frac{\partial}{\partial r}\left(1 - \frac{\partial\psi}{\partial r}\right) = \frac{1 + (2\alpha - 1)\,We\,\tau_{rr}}{(1 + We\,\tau_{rr})^2}\tau_{rx} \tag{34}$$

$$\frac{\partial}{\partial r}\left\{\frac{1}{(r+k)}\frac{\partial}{\partial r}[(r+k)^2\tau_{rx}]\right\} = \frac{M^2}{r+k}\frac{1 + (2\alpha - 1)\,We\,\tau_{rr}}{(1 + We\,\tau_{rr})^2}\tau_{rx} \tag{35}$$

In order to assess the accuracy of implemented method, above equations are solved directly in the absence of magnetic field and slip condition. Results showed to have great agreement with each other for the number of grid points used in FDM, i.e. $n = 1000$. In the absence of magnetic field and slip condition, the differential equation of shear stress could be solved directly, with two constants depending upon the stream function satisfying boundary conditions ($\tau_{rx} = c_1 + c_2/r^2$). Introducing τ_{rx} into governing equation of stream-function, the resulting equation can be solved using numerical integration techniques. We have used Gauss-Legendre Quadrature to evaluate the integral appearing in the solution of differential equation.

Results and Discussions

Figure 3-6 show the effects of different parameters on the behavior of a third order flow. For a constant flow rate, shear thickening behavior of fluid causes a greater pressure rise in the stream wise direction. In pumping region, curvature and magnetic field increase the stream wise pressure difference for low flow rates; while they have a reverse effect in co-pumping region. It is also observed that Knudsen number decreases the pressure difference.

Figure. 7-10 illustrate the effects of different parameters on the behaviour of a Giesekus flow. It should be noted that the effects of curvature, magnetic field, and Knudsen number on the Giesekus fluid is similar to the third order fluid. In contrast, the effect of elasticity decreases the pressure difference in pumping region.

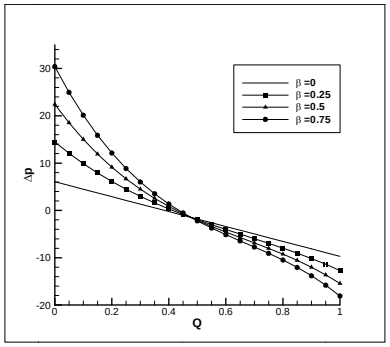

Figure 3. Variation of ΔP with flow rate for different values of β
$\phi = 0.4, k = 5, M = 4, Kn = 0.05$

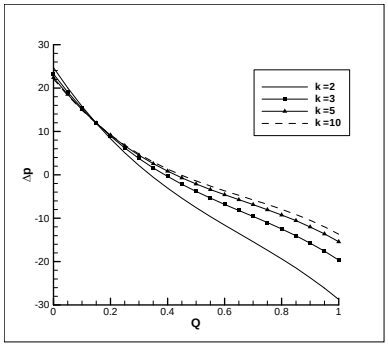

Figure 4. Variation of ΔP with flow rate for different values of k
$\phi = 0.4, \beta = 0.5, M = 4, Kn = 0.05$

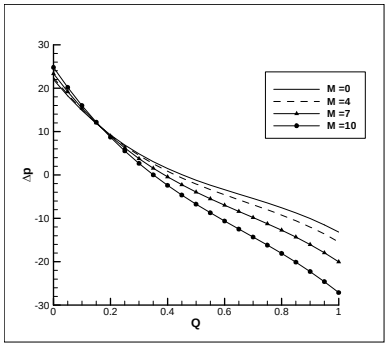

Figure 5. Variation of ΔP with flow rate for different values of M
$\phi = 0.4, k = 5, \beta = 0.5, Kn = 0.05$

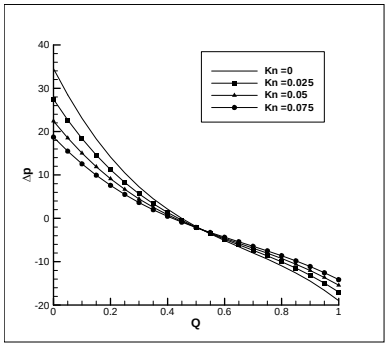

Figure 6. Variation of ΔP with flow rate for different values of Kn
$\phi = 0.4, k = 5, \beta = 0.5, M = 4$

Concluding and Remarks

Increase of the shear thickening behavior increases the pressure difference in pumping region even if the elasticity of the fluid has a reverse effect. The curvature and magnetic field enhance the pumping rate for both Giesekus and third Order fluid. Moreover, the Knudsen number decreases the pressure difference in pumping region for both considered fluids.

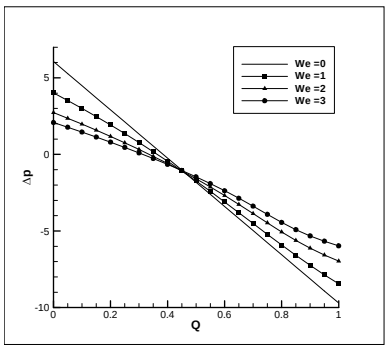

Figure 7. Variation of ΔP with flow rate for different values of We
$\phi = 0.4, k = 5, \alpha = 0.1, M = 4, Kn = 0.05$

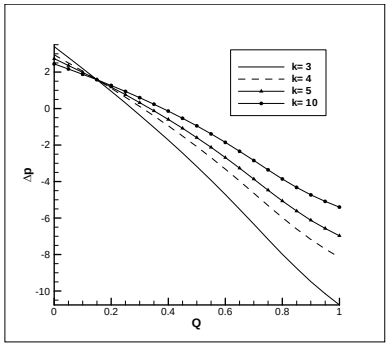

Figure 8. Variation of ΔP with flow rate for different values of k
$\phi = 0.4, \alpha = 0.1, We = 2, M = 4, Kn = 0.05$

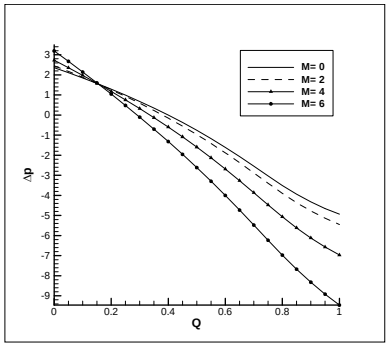

Figure 9. Variation of ΔP with flow rate for different values of M
$\phi = 0.4, k = 5, \alpha = 0.1, We = 2, Kn = 0.05$

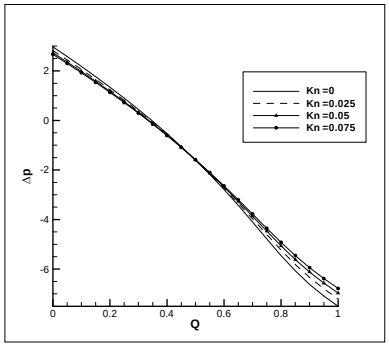

Figure 10. Variation of ΔP with flow rate for different values of Kn
$\phi = 0.4, k = 5, \alpha = 0.1, We = 2, M = 4$

References

[1] H. Sato, T. Kawai, T. Fujita, M. Okabe, Two dimensional peristaltic flow in curved channels, *Trans. The Japan Soc. Mech. Eng.* B 66 (2000) 679-685.

[2] N. Ali, M. Sajid, Z. Abbas, T. Javed, Non-Newtonian fluid flow induced by peristaltic waves in a curved channel, *Eur. J. Mech. B/Fluids* 29 (2010) 387–394.

[3] Rossow, V. J. "On flow of electrically conducting fluids over a flat plate in the presence of a transverse magnetic field." *NASA report No.* 1358 (1958): 489-508.

[4] H. Giesekus, A unified approach to a variety of constitutive models for polymer fluids based on the concept of configuration-dependent molecular mobility, *Rheol. Acta* 21 (1982) 366.

[5] Karniadakis G. E., Beskok A., Aluru N., *Microflows and Nanoflows*, Springer, 2005.

[6] Boyd, J. P., *Chebyshev and Fourier Spectral Method*, New York, Dover Publications, 2000.